

## Antiferroquadrupolar ordering and magnetic-field-induced phase transition in the cage compound $\text{PrRh}_2\text{Zn}_{20}$

Isao Ishii,\* Hitoshi Muneshige, Shuhei Kamikawa, Takahiro K. Fujita, Takahiro Onimaru, Naohiro Nagasawa, Toshiro Takabatake,<sup>†</sup> and Takashi Suzuki<sup>‡</sup>

*Department of Quantum Matter, ADSM, Hiroshima University, Higashi-Hiroshima 739-8530, Japan*

Genki Ano, Mitsuhiro Akatsu, Yuichi Nemoto, and Terutaka Goto

*Graduate School of Science and Technology, Niigata University, Niigata 950-2181, Japan*

(Received 3 November 2012; revised manuscript received 15 March 2013; published 7 May 2013)

To investigate the origin of a phase transition at  $T_Q = 0.06$  K simultaneously occurring with a superconducting transition in a cage compound  $\text{PrRh}_2\text{Zn}_{20}$ , we carried out ultrasonic measurements on a single-crystalline sample. The transverse modulus  $(C_{11} - C_{12})/2$  is intimately coupled to the non-Kramers ground doublet  $\Gamma_3$ , and elastic softening is observed at low temperatures. Below  $T_Q$ , the softening stops, suggesting the disappearance of quadrupole degrees of freedom. We clarified the negative quadrupole-quadrupole coupling constant and reentrant behavior of  $T_Q(H)$  in a magnetic field  $H$ . These results reveal that the phase transition at  $T_Q$  is antiferroquadrupolar ordering. The anisotropic magnetic field-temperature phase diagram is determined for  $H \parallel [100]$ ,  $[110]$ , and  $[111]$ . A magnetic-field-induced phase transition is newly found at high fields in all three field directions. We also observed ultrasonic dispersion at around 50 K owing to the rattling motion of Zn atoms at the 16c site, and pointed out the strong electron-phonon coupling in  $\text{PrRh}_2\text{Zn}_{20}$ .

DOI: [10.1103/PhysRevB.87.205106](https://doi.org/10.1103/PhysRevB.87.205106)

PACS number(s): 75.25.Dk, 62.20.de, 63.20.-e, 62.65.+k

### I. INTRODUCTION

In recent decades, exotic physical properties originating from localized  $f$  electrons, such as multipolar ordering, the (multichannel) Kondo effect, and the heavy-fermion superconductivity, have attracted much attention.<sup>1-3</sup> The orbital (electric quadrupole) degrees of freedom often play an important role for the understanding of their physical properties. Under a crystal electric field (CEF) in a cubic symmetry, the non-Kramers doublet  $\Gamma_3$  has the electric quadrupole and no magnetic dipole degrees of freedom, where  $\Gamma_i$  is the irreducible representation.

The cage compound  $RT_2\text{Zn}_{20}$  ( $R$ : rare earth,  $T$ : transition metal) has a cubic  $\text{CeCr}_2\text{Al}_{20}$ -type structure (space group  $Fd\bar{3}m$ ).<sup>4</sup> Onimaru *et al.* reported that  $\text{PrT}_2\text{Zn}_{20}$  undergoes a superconducting phase transition at  $T_{sc} = 0.05$  K ( $T = \text{Ir}$ ) and 0.06 K ( $T = \text{Rh}$ ) by their electrical resistivity and ac magnetic susceptibility measurements.<sup>5-7</sup> The superconductivity disappears under a magnetic field about 2 mT in both compounds.<sup>7,8</sup>  $\text{PrT}_2\text{Zn}_{20}$  also shows a phase transition at  $T_Q = 0.11$  K ( $T = \text{Ir}$ ) and 0.06 K ( $T = \text{Rh}$ ) other than the superconducting transition. In our previous study on  $\text{PrIr}_2\text{Zn}_{20}$ , we experimentally determined antiferroquadrupolar (AFQ) ordering at  $T_Q$  by using an ultrasonic technique.<sup>9</sup> The anisotropic magnetic field ( $H$ )-temperature ( $T$ ) phase diagram was also clarified for  $H \parallel [100]$ ,  $[110]$ , and  $[111]$ .

In  $\text{PrRh}_2\text{Zn}_{20}$ , the electrical resistivity shows a metallic behavior with hysteresis in the wide  $T$  range, suggesting a first-order phase transition at higher temperature than room temperature.<sup>7</sup> In x-ray diffraction experiments at low temperatures, however, there is no evidence of crystal-symmetry lowering from the cubic structure within the experimental resolution until now.<sup>10</sup> No lowering from the cubic symmetry is also suggested by the observation of CEF excitations in inelastic neutron-scattering experiments.<sup>11</sup>  $\text{PrRh}_2\text{Zn}_{20}$  appears

to retain the cubic structure even at low temperatures. The magnetic susceptibility  $\chi$  obeys the Curie-Weiss law above 30 K with the effective magnetic moment of the free  $\text{Pr}^{3+}$  ion. In specific-heat measurements, a Schottky anomaly is observed at 10 K and is reproduced by the ground doublet and an excited triplet separated by 31 K. These results reveal that the ground state under CEF is the non-Kramers doublet  $\Gamma_3$ . Onimaru *et al.* suggested that the phase transition at  $T_Q$  is AFQ ordering by their specific-heat measurements because  $T_Q$  tends to increase at low magnetic fields and anisotropic  $H$  dependence of  $T_Q$  is explained by assuming the molecular field of a quadrupole moment.<sup>7</sup> So far, there has been no experimental confirmation.

On the other hand, recently, a large-amplitude atomic motion of a guest atom, which is the so-called rattling motion, has been intensively investigated in cage compounds, such as the filled skutterudite.<sup>12</sup> In the  $RT_2\text{Zn}_{20}$  system, the Zn atom at the 16c site is accommodated in a polyhedral cage consisting of 2  $R$  atoms and 12 Zn atoms at the 96g site, as shown in the inset of Fig. 1. Atomic displacement parameters of Zn atom at the 16c site is the largest in x-ray diffraction experiments.<sup>4,10</sup> The Zn atom at the 16c site oscillates perpendicular to the La-Zn(16c)-La straight line in  $\text{LaRu}_2\text{Zn}_{20}$  by the calculation based on the first-principles method.<sup>13</sup> These results indicate that  $RT_2\text{Zn}_{20}$  has the rattling motion of Zn atoms at the 16c site. In ultrasonic measurements, ultrasonic dispersion (UD), which is ultrasonic frequency dependence of elastic moduli and ultrasonic attenuation, is observed at low temperatures in the filled skutterudite  $\text{RO}_4\text{Sb}_{12}$  and  $\text{RFe}_4\text{Sb}_{12}$ , and the clathrate  $\text{Ba}_8\text{Ga}_{16}\text{Sn}_{30}$ , for instance.<sup>14-17</sup> The UD can be explained as originating from the rattling motion of the guest atom in cage compounds.

Since a strain induced by ultrasound bilinearly couples to a corresponding quadrupole moment, the ultrasonic technique is a powerful tool for studying quadrupole degrees of freedom.

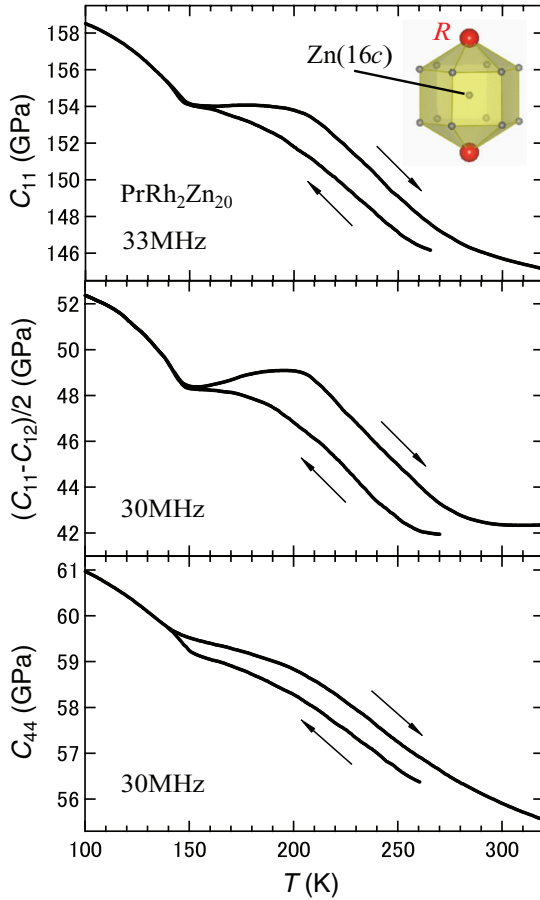


FIG. 1. (Color online)  $T$  dependencies of elastic moduli  $C_{11}$ ,  $(C_{11} - C_{12})/2$ , and  $C_{44}$  between 100 and 320 K in  $\text{PrRh}_2\text{Zn}_{20}$ . The inset shows the cage structure in the  $RT_2\text{Zn}_{20}$  system.

The elastic modulus  $(C_{11} - C_{12})/2$  is the linear response to  $\Gamma_3$  strain  $\varepsilon_{xx} - \varepsilon_{yy}$  in the cubic symmetry. If the non-Kramers doublet  $\Gamma_3$  is the ground state, remarkable elastic softening of  $(C_{11} - C_{12})/2$  is expected at low temperatures. In addition, the ultrasonic technique is quite useful to research the rattling motion as mentioned above. In this work, we performed ultrasonic measurements in order to clarify the origin of the phase transition at  $T_Q$  and the rattling motion in  $\text{PrRh}_2\text{Zn}_{20}$ .

## II. EXPERIMENT

A single crystal of  $\text{PrRh}_2\text{Zn}_{20}$  was grown by a Zn self-flux method.<sup>7</sup> The longitudinal elastic modulus  $C_{11}$  and the transverse moduli  $(C_{11} - C_{12})/2$  and  $C_{44}$  were measured as a function of  $T$  from 0.02 to 320 K using the phase-comparison-type pulse echo method.<sup>18</sup> Here,  $(C_{11} - C_{12})/2$  is the transverse mode propagating along the  $[110]$  axis with the polarization direction along the  $[110]$  axis. We also measured  $T$  and  $H$  dependencies of elastic moduli up to 14 T in  $H \parallel [100]$ ,  $[110]$ , and  $[111]$  using a superconducting magnet. To measure ultrasonic frequency dependence, we used the overtone of the fundamental resonance frequencies of  $\sim 30$  MHz of  $\text{LiNbO}_3$  transducers. The frequency range was between 30 and 232 MHz. An acoustic de Haas–van Alphen oscillation is observed in the  $H$  dependence of elastic moduli, indicating high purity of our sample.

## III. RESULTS AND DISCUSSION

### A. First-order phase transition at high temperature

Figure 1 shows  $T$  dependencies of elastic moduli  $C_{11}$ ,  $(C_{11} - C_{12})/2$ , and  $C_{44}$  above 100 K in  $\text{PrRh}_2\text{Zn}_{20}$ . All moduli increase with decreasing  $T$ . Above 150 K, obvious hysteresis over the wide  $T$  range is observed, indicating that there is a first-order phase transition at higher temperature than 320 K. This result is consistent with the data from the electrical resistivity.<sup>7</sup> Although the hysteresis disappears around 150 K, the specific heat shows no anomaly around 150 K. These facts suggest that there is no transition around 150 K, and 150 K is a simple end point of the large hysteresis. We estimate that the origin of the hysteresis may be a cubic-to-cubic transition because no lowering of crystal symmetry from the cubic structure is confirmed below 150 K so far in x-ray diffraction and inelastic neutron-scattering experiments within the experimental resolution.<sup>10,11</sup> Hereafter, we assume that  $\text{PrRh}_2\text{Zn}_{20}$  keeps the cubic structure even at very low temperatures.

### B. Antiferroquadrupolar ordering and ultrasonic dispersion

With further decrease in  $T$ , the moduli  $C_{11}$  and  $(C_{11} - C_{12})/2$  show an upturn at around 50 K, and then elastic softening is observed below 20 and 30 K, respectively, as shown in Fig. 2. The softening of  $C_{11}$  arises from that of  $(C_{11} - C_{12})/2$ .<sup>19,20</sup> In contrast, the modulus  $C_{44}$  exhibits no clear upturn at around 50 K and no elastic softening. All moduli show an upturn at around 2 K with further decreasing  $T$ . For the upturn at around 2 and 50 K, we measured all moduli at various ultrasonic frequencies and found UD, as shown in Fig. 3. These UD results in  $\text{PrRh}_2\text{Zn}_{20}$  will be discussed later. Since the data near 30 MHz are influenced by UD at around 2 K down to 0.1 K, we focus on the data near 100 MHz without the influence of UD below 1 K.  $C_{11}$  and  $(C_{11} - C_{12})/2$  near 100 MHz decrease again below 1 K. As shown in the insets of Fig. 2, the softening stops at  $T_Q$ , suggesting that most of the quadrupole degrees of freedom disappear at  $T_Q$ . At low temperatures, no hysteresis is observed in the  $T$  sweep.

Here, let us discuss the superconducting state in  $\text{PrRh}_2\text{Zn}_{20}$ . The superconducting transition occurs simultaneously at the same temperature with  $T_Q$  in zero field.<sup>7</sup> To examine an influence of the superconductivity, we measured the elastic moduli at the zero field (no remanent field of the superconducting magnet) and at very low fields (above 2 mT). However, no obvious difference is observed at around  $T_{sc}$  in our experimental resolution, suggesting a weaker coupling between the strain and a superconducting order parameter.

The softening of  $(C_{11} - C_{12})/2$  and no softening of  $C_{44}$  are clear evidence that the transition at  $T_Q$  is caused by the ground doublet  $\Gamma_3$ . We carried out a theoretical fitting between  $T_Q$  and 100 K for  $C_{11}$  and  $(C_{11} - C_{12})/2$  using a strain susceptibility  $\chi_s$  for the softening and a Debye-type relaxation for UDs. Concerning a quadrupole interaction, the symmetry about Pr is the cubic symmetry. We considered the effective Hamiltonian  $H_{\text{eff}}$ :

$$H_{\text{eff}} = H_{\text{CEF}} - g_{\Gamma_i} O_{\Gamma_i} \varepsilon_{\Gamma_i} - g'_{\Gamma_i} (O_{\Gamma_i}) O_{\Gamma_i},$$

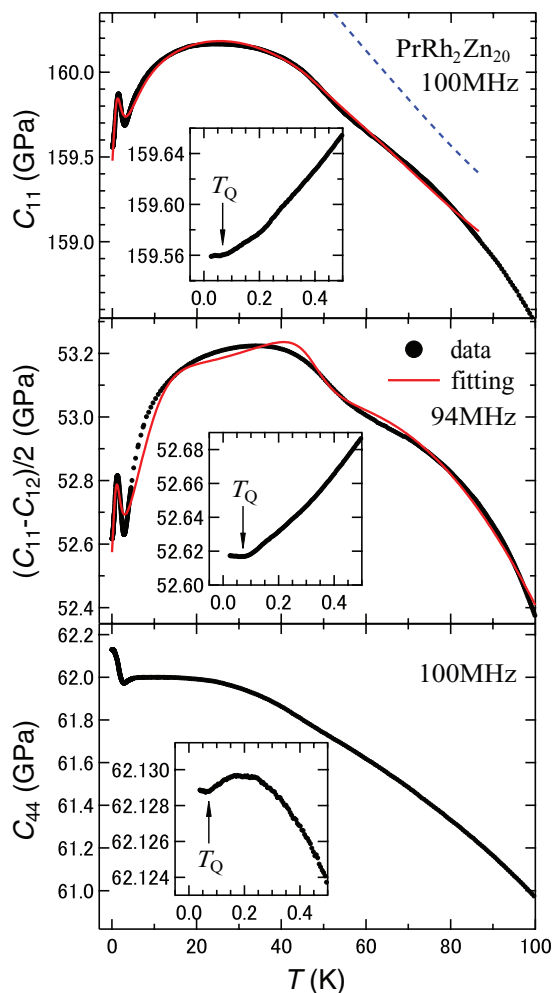


FIG. 2. (Color online)  $T$  dependencies of elastic moduli  $C_{11}$ ,  $(C_{11} - C_{12})/2$ , and  $C_{44}$  below 100 K in  $\text{PrRh}_2\text{Zn}_{20}$ , for ultrasonic frequencies near 100 MHz. The insets represent the same data in an expanded scale below 0.5 K. The red solid and blue dotted curves demonstrate the fitting result and the background stiffness, respectively. The background stiffness of  $(C_{11} - C_{12})/2$  is above the data.

$$H_{\text{CEF}} = W \left[ \frac{x}{60} (O_4^0 + 5O_4^4) + \frac{1 - |x|}{1260} (O_6^0 - 21O_6^4) \right],$$

where  $g_{\Gamma_i}$ ,  $g'_{\Gamma_i}$ ,  $W$ , and  $O_i^j$  are a strain-quadrupole coupling constant, a quadrupole-quadrupole coupling constant, a scale factor of CEF energy level, and the Stevens operator, respectively.<sup>21</sup>  $\langle O_{\Gamma_i} \rangle$  represents the thermal average of a quadrupole operator  $O_{\Gamma_i}$ . The  $T$  dependence of elastic modulus by the quadrupole interaction  $C_Q(T)$  is represented by the following equation:<sup>22</sup>

$$C_Q(T) = \frac{-N_0 g_{\Gamma_i}^2 \chi_s(T)}{1 - g'_{\Gamma_i} \chi_s(T)}, \quad (1)$$

where  $N_0 = 2.731 \times 10^{27} \text{ m}^{-3}$  is the number density of Pr ions per unit volume at room temperature. In addition to the quadrupole interaction, we employed a Debye-type formula

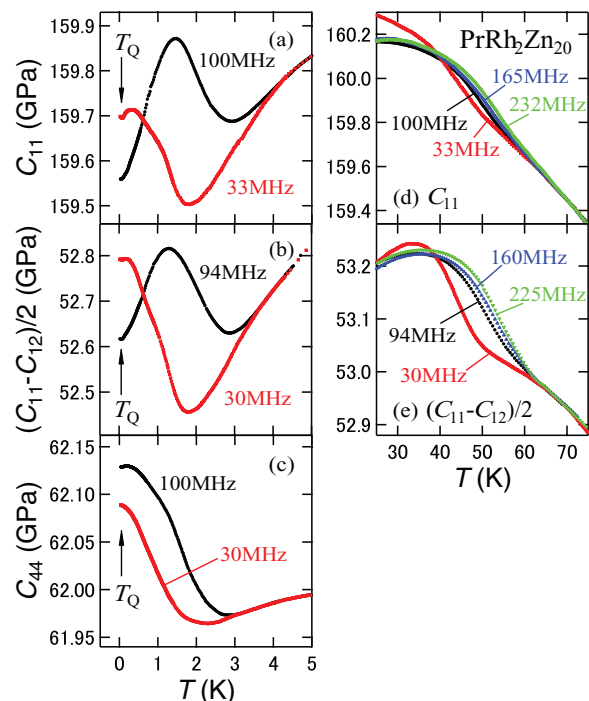


FIG. 3. (Color online) Frequency dependencies of elastic moduli around 2 K in (a)  $C_{11}$ , (b)  $(C_{11} - C_{12})/2$ , and (c)  $C_{44}$ , and around 50 K in (d)  $C_{11}$  and (e)  $(C_{11} - C_{12})/2$ .

and an Arrhenius-type relation for UDs:

$$C_{\text{UD}}(T) = \Delta C - \frac{\Delta C}{1 + \omega^2 \tau^2}, \quad \tau = \tau_0 \exp(E/T), \quad (2)$$

where  $\tau$  is a relaxation time,  $E$  is an activation energy,  $\omega$  is the angular frequency of the ultrasonic wave, and  $\Delta C$  is a difference between the elastic modulus of the high- and low-frequency limits. We assumed the background stiffness  $C_0(T) = a + bT^2 + cT^4$ .<sup>23</sup> The total elastic modulus using Eqs. (1) and (2) is as follows:

$$C(T) = C_Q(T) + C_{\text{UDL}}(T) + C_{\text{UDH}}(T) + C_0(T), \quad (3)$$

where the subscripts UDL and UDH denote UD at around 2 and 50 K, respectively.

The red solid curves in Fig. 2 are the best fit by using  $x = 0.46$ ,  $W = -1.1$ , and other fitting parameters listed in Tables I and II. In the fitting, we used the CEF level scheme proposed by specific heat, magnetization, and inelastic neutron-scattering experiments: the ground doublet  $\Gamma_3$ , the first excited triplet  $\Gamma_4$  at 31 K, and the second excited triplet  $\Gamma_5$  at 65 K.<sup>7,11</sup> There is a good agreement between the calculated  $C_{11}$  and the data. The softening and UDs in  $(C_{11} - C_{12})/2$  are well reproduced. The UD at around 2 K in  $C_{44}$  is also reproduced by the parameters listed in Table II. The negative  $g'$  and disappearance of the quadrupole degrees of freedom at  $T_Q$  indicate that the most plausible origin of the transition at  $T_Q$  is AFQ ordering.

The cage compounds, such as the filled skutterudites  $\text{PrOs}_4\text{Sb}_{12}$  and  $\text{LaFe}_4\text{Sb}_{12}$ , show UD at several dozen kelvin originating from the rattling motion of the guest atom.<sup>14,16</sup> As mentioned in Sec. I,  $\text{RT}_2\text{Zn}_{20}$  has the rattling motion of Zn atoms at the 16c site. In  $\text{PrRh}_2\text{Zn}_{20}$ , UD at around 50 K is caused by the rattling motion of Zn atoms at the 16c

TABLE I. Fitting parameters of elastic moduli  $|g|$  (K),  $g'$  (K),  $a$  (GPa),  $b$  ( $\times 10^{-4}$  GPa/K<sup>2</sup>),  $c$  ( $\times 10^{-9}$  GPa/K<sup>4</sup>), and  $\Delta C$  (GPa).

	$ g $	$g'$	$a$	$b$	$c$	$\Delta C$ (UDL)	$\Delta C$ (UDH)
$C_{11}$	102.8	-0.138	160.8	-3.256	0.129	1.503	0.056
$(C_{11} - C_{12})/2$	920.8	-2.328	65.08	-2.413	0.018	1.000	0.220

site because the temperature of UD is very similar to that of the filled skutterudites. Hereafter, we discuss the origin of UD at around 50 K in PrRh<sub>2</sub>Zn<sub>20</sub>. In phonon dispersion curves of cage compounds, there is a low-lying flat optical phonon branch owing to the rattling motion reported by inelastic x-ray and neutron-scattering experiments.<sup>24,25</sup> We previously pointed out that UD in cage compounds is caused by a coupling between an acoustic phonon and the low-lying optical phonon interacting with electrons around the Fermi energy  $E_F$  by using the results of ultrasonic measurements and band calculation in LaM<sub>4</sub>Sb<sub>12</sub> ( $M = \text{Fe, Ru, and Os}$ ), and the theory by Hattori and Miyake.<sup>16,26</sup> The appearance tendency of UD is directly related to the strength of electron-phonon coupling. The coupling is proportional to  $g_{e-p}^2 N_F$  in the theory, where  $g_{e-p}$  is an electron-phonon coupling constant and  $N_F$  is the number of states at  $E_F$ . In the isomorphous compound LaRu<sub>2</sub>Zn<sub>20</sub>, calculated results based on the first-principles method reveal low-lying optical phonon branches.<sup>27</sup> The UD at around 50 K originates from a larger  $g_{e-p}^2 N_F$ , suggesting the strong electron-phonon coupling in PrRh<sub>2</sub>Zn<sub>20</sub>.

UD is observed at two different temperatures (around 2 and 50 K) in PrRh<sub>2</sub>Zn<sub>20</sub>. These behaviors are also reported in the filled skutterudites RO<sub>4</sub>Sb<sub>12</sub>.<sup>15</sup> However,  $E$  obtained from UD at around 2 K is very low compared with the filled skutterudite compounds. Although the origin of UD at around 2 K is unclear at present, a possible origin will be discussed in Sec. III D.

### C. Magnetic field-temperature phase diagram

To investigate a  $H$ - $T$  phase diagram of the ordered state in PrRh<sub>2</sub>Zn<sub>20</sub>, we carried out ultrasonic measurements under magnetic fields at ultrasonic frequencies near 100 MHz without the influence of UD below 1 K. We detected clear acoustic de Haas-van Alphen oscillations, revealing that there are small extremal orbits with the frequencies 145, 142, and 149 T perpendicular to [100], [110], and [111] directions, respectively. We first present a clear phase boundary of  $T_Q$  in  $H \parallel [110]$  and [111]. Figures 4 and 5 show  $(C_{11} - C_{12})/2$  in  $H \parallel [110]$  and [111], respectively. At zero field, softening of  $(C_{11} - C_{12})/2$  stops at  $T_Q$ . Above 2 T,  $(C_{11} - C_{12})/2$  shows a broad minimum, and then an inflection point is observed below the temperature of the minimum in both  $H \parallel [110]$  and [111], as shown in Figs. 4(a) and 5(a), respectively. The temperature of the inflection point corresponds to that

 TABLE II. Fitting parameters  $\tau_0$  ( $\times 10^{-11}$  s) and  $E$  (K).

	UDL	UDH
$\tau_0$	80.0	0.02
$E$	2.50	440

of the peak in the specific heat.<sup>7</sup> We defined the inflection point and the minimum of the data above 2 T as  $T_Q$  and  $T^*$ , respectively.  $T_Q$  increases with increasing  $H$  in both  $H \parallel [110]$  and [111]. The highest  $T_Q$  is 0.126 K in  $H \parallel [110]$  and 0.135 K in  $H \parallel [111]$  at 7 T.  $T_Q$  decreases gradually with further increasing  $H$ , and then  $T_Q$  becomes unclear above 9 T. In the  $H$  dependencies of  $(C_{11} - C_{12})/2$  shown in Figs. 4(b) and 5(b), elastic softening is observed above 4 T. With further increase in  $H$ , the softening is reduced at 11.7 T in  $H \parallel [110]$  and stops at 12.9 T in  $H \parallel [111]$ . We determined phase boundaries from  $T$  dependencies (closed circles) and  $H$  dependencies (closed diamonds) of the elastic moduli in  $H \parallel [110]$  and [111], as shown in Figs. 4(c) and 5(c), respectively. These reentrant behaviors of  $T_Q$ , that is consistent with the results from specific-heat measurements performed below 7 T, are similar to the AFQ phase diagram in PrIr<sub>2</sub>Zn<sub>20</sub> and PrPb<sub>3</sub>.<sup>7,9,28,29</sup> The phase diagrams of  $T_Q$  in PrRh<sub>2</sub>Zn<sub>20</sub> also indicate that the transition at  $T_Q$  is AFQ ordering. Onimaru *et al.* suggested that an antiferromagnetic interaction between the magnetic dipoles induced by  $H$  stabilizes the AFQ ordering.<sup>7</sup>

Here,  $T^*$  (minimum of the data; closed triangles in the phase diagram) also increases with increasing  $H$  and is the highest at 7 T, as shown in Figs. 4(c) and 5(c).  $T^*$  decreases

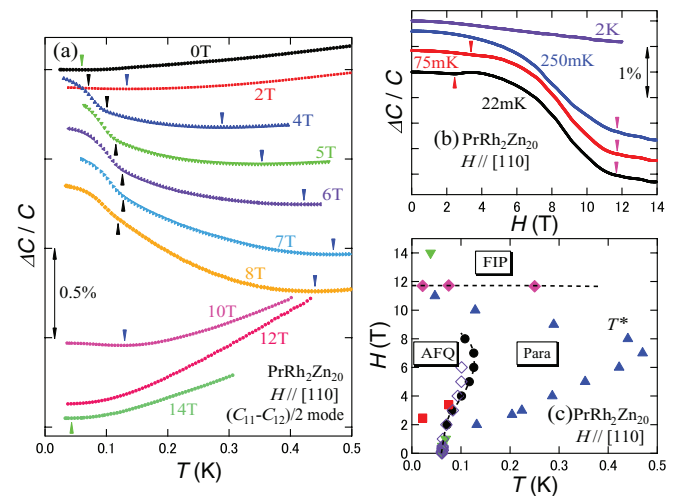


FIG. 4. (Color online) (a)  $T$  dependencies of  $(C_{11} - C_{12})/2$  in  $H \parallel [110]$ . (b)  $H$  dependencies of  $(C_{11} - C_{12})/2$  at each fixed  $T$ . We plotted the data adding constant value to easily see each data curve. (c) The  $H$ - $T$  phase diagram in  $H \parallel [110]$ . The phase boundaries are estimated from the  $T$  dependencies (closed circles) and  $H$  dependencies (closed diamonds) of the elastic moduli. The broken curves are guides for the eyes. Open diamonds show the phase boundary obtained from specific-heat measurements (Ref. 7). Closed triangles denote the minimum of the  $T$  dependence explained in the text in detail.

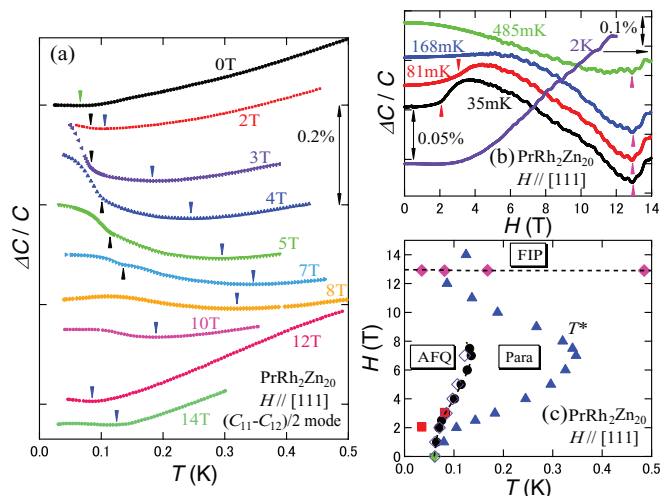


FIG. 5. (Color online) (a)  $T$  dependencies of  $(C_{11} - C_{12})/2$  in  $H \parallel [111]$ . (b)  $H$  dependencies of  $(C_{11} - C_{12})/2$  at each fixed  $T$ . We plotted the data adding constant value to easily see each data curve. (c) The  $H$ - $T$  phase diagram in  $H \parallel [111]$ . The broken curves are guides for the eyes.

with further increase in  $H$ . These behaviors of  $T^*$  are almost the same as those of  $T_Q$ . In contrast, no anomaly is observed at  $T^*$  in the specific heat, suggesting that there is no phase transition at  $T^*$ . The origin of  $T^*$  is unclear at present, however,  $T^*$  would correlate with  $T_Q$ . On the other hand, closed squares in the phase diagrams address a bend in the  $H$  dependencies of elastic moduli. These are observed in the ordered state, suggesting slight modulation of the AFQ state.

The modulus  $C_{11}$  in  $H \parallel [100]$  is shown in Fig. 6.  $T_Q$  at which softening of  $C_{11}$  stops is hardly changed by  $H$  below 2 T and becomes unclear above 3 T, as shown in

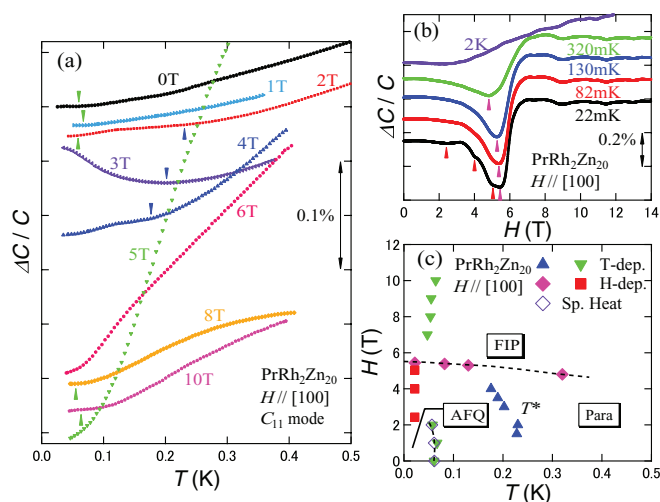


FIG. 6. (Color online) (a)  $T$  dependencies of  $C_{11}$  in  $H \parallel [100]$ . (b)  $H$  dependencies of  $C_{11}$  at each fixed  $T$ . We plotted the data adding constant value to easily see each data curve. (c) The  $H$ - $T$  phase diagram in  $H \parallel [100]$ . The broken curves are guides for the eyes.

Fig. 6(a).  $T^*$  is also observed in  $H \parallel [100]$ . The magnitude of softening increases with increasing  $H$  and is the largest at 5 T. Figure 6(b) shows the  $H$  dependencies of  $C_{11}$ . A peak structure is observed at around 5 T even at 320 mK (above  $T_Q$ ) in contrast to  $C_{11}$  at 2 K without the peak. The peak indicates a magnetic-field-induced phase transition at very low temperatures. In the  $H$  dependencies of  $(C_{11} - C_{12})/2$  in  $H \parallel [110]$  and  $[111]$  shown in Figs. 4(b) and 5(b), respectively,  $(C_{11} - C_{12})/2$  shows a reduction of the softening at 11.7 T in  $H \parallel [110]$  and a peak structure at 12.9 T in  $H \parallel [111]$  even above  $T_Q$ . From these results, we found a new phase boundary induced by  $H$  and defined the high-field phase as the magnetic-field-induced phase (FIP) discussed in the next section in detail. Thus, we clarified the  $H$ - $T$  phase diagram for all three field directions in  $\text{PrRh}_2\text{Zn}_{20}$ .

#### D. Magnetic-field-induced phase transition

We discuss the FIP transition observed along all field directions by using the data of  $C_{11}$  in  $H \parallel [100]$  for instance. In the  $H$  dependencies of  $C_{11}$  shown in Fig. 6(b), elastic softening turns into hardening at around 5 T even at 320 mK. In contrast, monotonic hardening is observed at 2 K, indicating that the FIP transition disappears below 2 K. The ground doublet  $\Gamma_3$  is isolated below 2 K because the first excited triplet  $\Gamma_4$  exists at 31 K in  $\text{PrRh}_2\text{Zn}_{20}$ . The FIP transition seems to occur around a magnetic field at which both  $T^*$  and  $T_Q$  are getting closer to zero. In the  $H$  dependencies of the CEF level scheme calculated, a splitting of the ground doublet  $\Gamma_3$  by the Zeeman effect in  $H \parallel [100]$  is larger than that in  $H \parallel [110]$  and  $[111]$ . The quadrupole interaction rapidly decreases with increasing  $H \parallel [100]$  compared with  $H \parallel [110]$  and  $[111]$ . The magnetic field where the FIP transition appears in  $H \parallel [100]$  (around 5 T) is lower than that in  $H \parallel [110]$  and  $[111]$  (around 12 T). These results suggest that the quadrupole degrees of freedom of the ground doublet  $\Gamma_3$  play an important role for the FIP transition. On the other hand, the  $T$  dependence of  $C_{11}$  at 5 T near the FIP boundary shows significantly larger softening than  $C_{11}$  at 0 T, as shown in Fig. 6(a). The softening of  $C_{11}$  at 5 T continues down to 40 mK as if it suggests that the transition temperature becomes zero. There is a possibility that the FIP transition includes a quantum criticality based on quadrupole fluctuations.

To check whether the  $H$  dependencies of  $C_{11}$  are reproduced by a simple localized (CEF) model of  $4f$  electrons, we performed a theoretical calculation for  $C_{11}$  using the CEF level and  $g'$ . The  $H$  dependence of the calculated  $C_{11}$  shows elastic hardening at very low temperatures because the quadrupole interaction is reduced by the splitting of the ground doublet  $\Gamma_3$  with increasing  $H$ . Hardening in the data at 2 K, where the FIP boundary vanishes, is consistent with the calculated  $C_{11}$ . However, the data of  $C_{11}$  below 320 mK exhibit elastic softening below 5 T. The simple localized model of  $4f$  electrons can not explain the softening. The mysterious softening below the FIP boundary is also observed in the  $H$  dependencies of  $(C_{11} - C_{12})/2$  in  $H \parallel [110]$  and  $[111]$ . Moreover, the isomorphous compound  $\text{PrIr}_2\text{Zn}_{20}$  with the  $\Gamma_3$  ground doublet shows almost the same behaviors.<sup>9</sup>

We point out a possible candidate for the phase below the FIP boundary from the viewpoint of a vibronic state (VS),

which arises from a coupling between degenerate  $f$ -electron orbitals and dynamical Jahn-Teller (JT) phonons.<sup>30,31</sup> In the theory by Hotta, dynamical JT phonons enhance the quadrupole fluctuations in VS accompanied by the entropy release of  $R \ln 2$ , where  $R$  is the gas constant. The VS is suggested in  $\text{PrMg}_3$  with the  $\Gamma_3$  ground doublet.<sup>32</sup>  $\text{PrMg}_3$  has no phase transition and gradually releases electronic entropy of the  $\Gamma_3$  ground doublet by VS.<sup>33</sup> Ultrasonic frequency dependence is observed at around 0.2 K and is explained to originate from VS in  $\text{PrMg}_3$  ( $\tau_0 = 8.5 \times 10^{-10}$  s and  $E = 0.5$  K).<sup>32</sup> In  $\text{PrRh}_2\text{Zn}_{20}$  and  $\text{PrIr}_2\text{Zn}_{20}$ , released entropy is only  $0.1R \ln 2$  and  $0.2R \ln 2$ , respectively, at  $T_Q$  and reaches  $R \ln 2$  at around 2 K.<sup>6,7</sup> Both  $\text{PrRh}_2\text{Zn}_{20}$  and  $\text{PrIr}_2\text{Zn}_{20}$  show UD at around 2 K. The parameters  $\tau_0$  ( $=8.0 \times 10^{-10}$  s) and  $E$  ( $=2.5$  K) in  $\text{PrRh}_2\text{Zn}_{20}$  are the same order of those in  $\text{PrMg}_3$ . If both compounds have VS of the Pr atom, a rotational motion among equivalent positions exists and a doubly degenerate state is formed. The VS includes electronic states with the  $E_g$  corresponding to  $(C_{11} - C_{12})/2$  and  $T_{2g}$  ( $C_{44}$ ) modes. There is a possibility that these electronic states interact with the strain induced by ultrasound and UD at around 2 K is an indication of VS. We propose that both compounds have VS at very low temperatures in addition to the long-range quadrupole interaction.

The mysterious softening stops at the FIP transition. The VS may break at the transition because doubly degenerate rotational modes of VS can be lifted by the magnetic field. Consequently, the FIP should become a simple multipole-

interaction phase. To clarify the origin of the FIP transition, further experimental and theoretical studies are needed.

#### IV. CONCLUSION

We measured the elastic moduli of  $\text{PrRh}_2\text{Zn}_{20}$  with the non-Kramers ground doublet  $\Gamma_3$ . The electric quadrupole degrees of freedom disappear at  $T_Q$  and the quadrupole-quadrupole coupling constant is negative in  $(C_{11} - C_{12})/2$ . We found anisotropic  $H$  dependence for three field directions and the reentrant behavior of  $T_Q$ . From these results, we experimentally determined that the phase transition at  $T_Q$  is AFQ ordering. We also clarified the magnetic-field-induced phase transition originating from the quadrupole degrees of freedom of the ground doublet  $\Gamma_3$  for all field directions. The elastic moduli show ultrasonic dispersion at around 2 and 50 K. We proposed that the ultrasonic dispersion at around 50 K is caused by the rattling motion of Zn atoms at the  $16c$  site due to the strong electron-phonon coupling.

#### ACKNOWLEDGMENTS

The authors would like to thank T. Hasegawa, Y. Matsushita, and K. Iwasa for helpful discussions. This work was supported by a Grant-in-Aid for Scientific Research on Innovative Areas ‘‘Heavy Electrons’’ (Grant No. 20102005) from the Ministry of Education, Culture, Sports, Science, and Technology of Japan.

\*ish@hiroshima-u.ac.jp

<sup>†</sup>Also at Institute for Advanced Materials Research, Hiroshima University.

<sup>‡</sup>Also at Institute for Advanced Materials Research, and Cryogenics and Instrumental Analysis Division, N-BARD, Hiroshima University; tsuzuki@hiroshima-u.ac.jp

<sup>1</sup>P. Morin and D. Schmitt, in *Ferromagnetic Materials*, edited by K. H. J. Buschow and E. P. Wohlfarth, Vol. 5 (Elsevier, Amsterdam, 1990), Chap. 1.

<sup>2</sup>D. L. Cox, *Phys. Rev. Lett.* **59**, 1240 (1987).

<sup>3</sup>E. D. Bauer, N. A. Frederick, P. C. Ho, V. S. Zapf, and M. B. Maple, *Phys. Rev. B* **65**, 100506(R) (2002).

<sup>4</sup>T. Nasch, W. Jeitschko, and U. C. Rodewald, *Z. Naturforsch. B Chem. Sci.* **52**, 1023 (1997).

<sup>5</sup>T. Onimaru, K. T. Matsumoto, Y. F. Inoue, K. Umeo, Y. Saiga, Y. Matsushita, R. Tamura, K. Nishimoto, I. Ishii, T. Suzuki, and T. Takabatake, *J. Phys. Soc. Jpn.* **79**, 033704 (2010).

<sup>6</sup>T. Onimaru, K. T. Matsumoto, Y. F. Inoue, K. Umeo, T. Sakakibara, Y. Karaki, M. Kubota, and T. Takabatake, *Phys. Rev. Lett.* **106**, 177001 (2011).

<sup>7</sup>T. Onimaru, N. Nagasawa, K. T. Matsumoto, K. Wakiya, K. Umeo, S. Kittaka, T. Sakakibara, Y. Matsushita, and T. Takabatake, *Phys. Rev. B* **86**, 184426 (2012).

<sup>8</sup>M. Matsushita, J. Sakaguchi, Y. Taga, M. Ohya, S. Yoshiuchi, H. Ota, Y. Hirose, K. Enoki, F. Honda, K. Sugiyama, M. Hagiwara, K. Kindo, T. Tanaka, Y. Kubo, T. Takeuchi, R. Settai, and Y. Ōnuki, *J. Phys. Soc. Jpn.* **80**, 074605 (2011).

<sup>9</sup>I. Ishii, H. Muneshige, Y. Suetomi, T. K. Fujita, T. Onimaru, K. T. Matsumoto, T. Takabatake, K. Araki, M. Akatsu, Y. Nemoto, T. Goto, and T. Suzuki, *J. Phys. Soc. Jpn.* **80**, 093601 (2011).

<sup>10</sup>Y. Matsushita (private communication).

<sup>11</sup>K. Iwasa (private communication).

<sup>12</sup>B. C. Sales, D. Mandrus, and R. K. Williams, *Science* **272**, 1325 (1996).

<sup>13</sup>T. Hasegawa, N. Ogita, and M. Udagawa, *J. Phys.: Conf. Ser.* **391**, 012016 (2012).

<sup>14</sup>T. Goto, Y. Nemoto, K. Sakai, T. Yamaguchi, M. Akatsu, T. Yanagisawa, H. Hazama, K. Onuki, H. Sugawara, and H. Sato, *Phys. Rev. B* **69**, 180511(R) (2004).

<sup>15</sup>T. Yanagisawa, Y. Ikeda, H. Saito, H. Hidaka, H. Amitsuka, K. Araki, M. Akatsu, Y. Nemoto, T. Goto, P. Ho, R. E. Baumbach, and M. B. Maple, *J. Phys. Soc. Jpn.* **80**, 043601 (2011).

<sup>16</sup>I. Ishii, T. Fujita, I. Mori, H. Sugawara, M. Yoshizawa, K. Takegahara, and T. Suzuki, *J. Phys. Soc. Jpn.* **78**, 084601 (2009).

<sup>17</sup>I. Ishii, Y. Suetomi, T. K. Fujita, K. Suekuni, T. Tanaka, T. Takabatake, T. Suzuki, and M. A. Avila, *Phys. Rev. B* **85**, 085101 (2012).

<sup>18</sup>T. J. Moran and B. Lüthi, *Phys. Rev.* **187**, 710 (1969).

<sup>19</sup>T. Suzuki, I. Ishii, N. Okuda, K. Katoh, T. Takabatake, T. Fujita, and A. Tamaki, *Phys. Rev. B* **62**, 49 (2000).

<sup>20</sup>S. Nakamura, T. Goto, O. Suzuki, S. Kunii, and S. Sakatsume, *Phys. Rev. B* **61**, 15203 (2000).

<sup>21</sup>K. R. Lea, M. J. M. Leask, and W. P. Wolf, *J. Phys. Chem. Solids* **23**, 1381 (1962).

- <sup>22</sup>B. Lüthi, in *Dynamical Properties of Solids*, edited by G. K. Horton and A. A. Maradudin (North-Holland, Amsterdam, 1980), Chap. 4.
- <sup>23</sup>M. Nohara, T. Suzuki, Y. Maeno, T. Fujita, I. Tanaka, and H. Kojima, *Phys. Rev. B* **52**, 570 (1995).
- <sup>24</sup>M. Christensen, A. B. Abrahamsen, N. B. Christensen, F. Juranyi, N. H. Andersen, K. Lefmann, J. Andreasson, C. R. H. Bahl, and B. B. Iversen, *Nat. Mater.* **7**, 811 (2008).
- <sup>25</sup>C. H. Lee, I. Hase, H. Sugawara, H. Yoshizawa, and H. Sato, *J. Phys. Soc. Jpn.* **75**, 123602 (2006).
- <sup>26</sup>K. Hattori and K. Miyake, *J. Phys. Soc. Jpn.* **76**, 094603 (2007).
- <sup>27</sup>T. Hasegawa (private communication).
- <sup>28</sup>T. Tayama, T. Sakakibara, K. Kitami, M. Yokoyama, K. Tenya, H. Amitsuka, D. Aoki, Y. Ōnuki, and Z. Kletowski, *J. Phys. Soc. Jpn.* **70**, 248 (2001).
- <sup>29</sup>T. Sakakibara, T. Tayama, T. Onimaru, D. Aoki, Y. Onuki, H. Sugawara, Y. Aoki, and H. Sato, *J. Phys.: Condens. Matter* **15**, S2055 (2003).
- <sup>30</sup>T. Hotta, *Phys. Rev. Lett.* **96**, 197201 (2006).
- <sup>31</sup>T. Hotta, *J. Phys. Soc. Jpn.* **76**, 023705 (2007).
- <sup>32</sup>K. Araki, T. Goto, K. Mitsumoto, Y. Nemoto, M. Akatsu, H. S. Suzuki, H. Tanida, S. Takagi, S. Yasin, S. Zherlitsyn, and J. Wosnitzer, *J. Phys. Soc. Jpn.* **81**, 023710 (2012).
- <sup>33</sup>H. Tanida, H. S. Suzuki, S. Takagi, H. Onodera, and K. Tanigaki, *J. Phys. Soc. Jpn.* **75**, 073705 (2006).